die Angabe für die Mantelkomponente eine obere Grenze dar, da auch Nachentladungen durch das Gegenfeld unterdrückt werden. So dürfte der steilere Anstieg bei höheren Arbeitsspannungen im wesentlichen auf die Zunahme der Nachentladungen zurückzuführen sein. Dafür spricht auch die bekannte Verbesserung der Zählrohr-Plateaus durch Unterdrückung der Nachentladungen durch eine genügend lange künstliche Totzeit.

Die Untersuchung wird fortgesetzt.

Diese Arbeit wurde unter Verwendung von Mitteln der Deutschen Forschungsgemeinschaft durchgeführt.

Numerical Calculation of the Potential Distribution in Ion Slit Lens Systems I

By A. J. H. Boerboom

F.O.M.-Laboratorium voor Massaspectrografie, Amsterdam, Netherlands

(Z. Naturforschg. **14 a**, 809—816 [1959]; eingegangen am 18. April 1959)

The potential distribution is calculated in an ion lens, consisting of three parallel collinear slits in three parallel electrodes. The slit system is supposed to be infinite in the direction of the slits, so the problem becomes two dimensional in a plane perpendicular on the direction of the slits. In this plane the potential distribution is calculated by the method of conformal transformation.

The Schwarz–Christoffel transformation is used to map conformally the region between the projections of the electrodes of the slit system. It proves to be very simple to perform this transformation. Formulae are given for the case of an ion lens consisting of slits in three parallel plates. A series expansion and an iteration method are developed to find the necessary parameters. Both methods prove to be satisfactory if the slit widths are smaller than the distance to the neighbouring electrodes. Symmetrical lenses, not satisfying this condition will be treated in a second paper. In a third paper slit system will be treated with an arbitrary number of electrodes.

In the transformed region Laplace's equation is solved, having as boundary conditions the potentials on the electrodes. In this way the exact potential distribution in the lens system is found. In a typical example the potential distributions are calculated along the axis for several potentials on the electrodes, together with the corresponding fields.

To compute the potential distribution in a lens system, Laplace's equation

$$\Delta V = 0 \qquad (1)$$

is to be solved. The boundary conditions are set by the potentials at the electrodes and the field strength at infinity.

In literature only a few simple cases are treated. E. g. Henneberg [1] and Glaser and Henneberg [2] treat the case of one thin electrode at zero potential, with the field strengths at infinity as boundary conditions, in which electrode they assume either an infinitely long slit or a circular hole. In the present paper multiple electrode configurations are treated. The electrodes and slits are assumed to be of infinite length, so the problem can be considered two dimensional in a plane perpendicular on the direction of the slits. As this boundary is rather complicated, the region between the projections of the slits is mapped conformally on the positive imaginary half of a complex plane, so that the electrode configuration falls along the real axis. This is the so called Schwarz–Christoffel transformation [3]. Over this transformtion Laplace's equation is invariant, so in the new plane the same equation is to be solved, with much simpler boundary conditions.

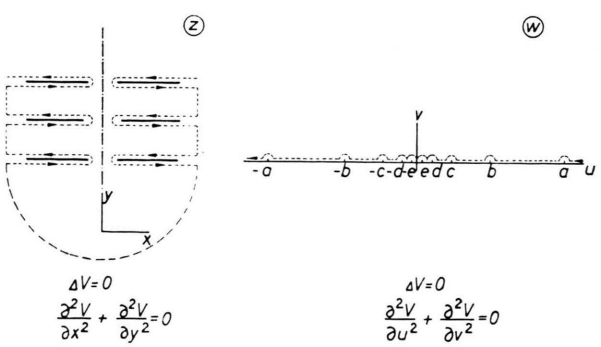

Fig. 1. Conformal mapping.

As the Schwarz–Christoffel transformation is suitable for any region bounded by straight lines,

[1] W. Henneberg, Z. Phys. **94**, 22 [1935].
[2] A. Glaser and W. Henneberg, Z. techn. Phys. **16**, 222 [1935].
[3] P. M. Morse and H. Feshbach, Methods of Theoretical Physics I, New York 1953, p. 445.

the method to be developed in this paper is quite generally applicable. We confine ourselves however, to lenses consisting of three slits in three parallel electrodes. The slits are assumed to be parallel with collinear centres, the connecting line being a line of symmetry of the lens system.

§ 1. Performance of the transformation

The thickness of the electrodes is neglected in the first instance to get the configuration of Fig. 2. Let the slit widths be respectively $2s_1$, $2s_2$ and $2s_3$; the electrode distances πr_1 and πr_2.

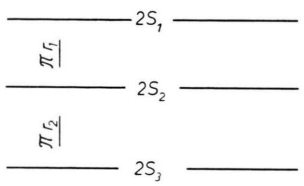

Fig. 2. Three electrode lens.

This electrode configuration is considered as a degenerate polygon in the complex z-plane ($z = x + iy$). The conformal mapping of this z-plane to a complex w-plane ($w = u + iv$) is performed by the inverse of the function:

$$z = \int_{w_0}^{w} \frac{(s^2-a^2)(s^2-c^2)(s^2-e^2)}{(s^2-b^2)(s^2-d^2)s^2}\,ds$$
$$= w + B\ln\frac{w-b}{w+b} + D\ln\frac{w-d}{w+d} + \frac{E}{w} + \text{const} \qquad (2)$$

with $B = \dfrac{(b^2-a^2)(b^2-c^2)(b^2-e^2)}{2b(b^2-d^2)b^2}$;

$$D = \frac{(d^2-a^2)(d^2-c^2)(d^2-e^2)}{2d(d^2-b^2)d^2}; \quad E = \frac{a^2c^2e^2}{b^2d^2}.$$

a, b, c, d, and e are real constants, satisfying the conditions

$$a > b > c > d > e > 0.$$

These constants have still to be determined.

The following consideration shows, that the function (2) does indeed map the u-axis in the w-plane on the electrode configuration:

If s lies on the positive u-axis, with $s > a$, the integrand is positive. If s decreases, then ds is negative, so x also decreases and the image of a point moving along the u-axis describes a line parallel to the real axis of the z-plane. For $s = a$ the integrand changes sign and the image point will move along the same line parallel to the x-axis in the opposite direction. For $w \to b + 0$ x goes to plus infinity. To avoid this difficulty the point in the w-plane is assumed to describe a small semi-circle round $s = b$:

$$s = b + r e^{i\varphi}, \qquad 0 \le \varphi \le \pi.$$

The corresponding change in the z-plane is given by

$$z(w = b-0) - z(w = b+0)$$
$$= \lim_{r\to 0}\int_0^{\pi}\left\{1 + \frac{B}{r e^{i\varphi}} + \ldots\right\} r e^{i\varphi}\,d\varphi = B i \pi,$$

so the image point moves over a distance of $B\pi$ in the direction perpendicular to the real axis. When w moves from b to c, the image point describes half of a line parallel to the first at a distance $B\pi$ from it. So it is obvious that the image point of a point moving along the u-axis describes the electrode configuration in the z-plane. The coefficients B and D are determined by the distances of the electrodes.

The slit width of the first slit is given by

$$2s_1 = \Re e\, z(w = a) - \Re e\, z(w = -a)$$
$$= \Re e\,\{z(w = a) - z(w = -a)\}$$
$$= 2\left\{a + B\ln\frac{a-b}{a+b} + D\ln\frac{a-d}{a+d} + \frac{E}{a}\right\}.$$

The two distances between the electrodes and the three slit widths furnish the five equations to determine a, b, c, d, and e.

§ 2. Approximate solution

The equations to determine the parameters governing the conformal mapping are

$$\left.\begin{aligned}
&a + r_1\ln\frac{a+b}{a-b} + r_2\ln\frac{a+d}{a-d} + \frac{a\,c^2\,e^2}{b^2\,d^2} = s_1,\\
&\frac{a^2-b^2}{2b}\,\frac{b^2-c^2}{b^2-d^2}\,\frac{b^2-e^2}{b^2} = r_1,\\
&c + r_1\ln\frac{b+c}{b-c} + r_2\ln\frac{c+d}{c-d} + \frac{a^2\,c\,e^2}{b^2\,d^2} = s_2,\\
&\frac{c^2-d^2}{2d}\,\frac{a^2-d^2}{b^2-d^2}\,\frac{d^2-e^2}{d^2} = r_2,\\
&e + r_1\ln\frac{b+e}{b-e} + r_2\ln\frac{d+e}{d-e} + \frac{a^2\,c^2\,e}{b^2\,d^2} = s_3.
\end{aligned}\right\} \qquad (3)$$

From these five equations the five unknowns have to be solved, where it is known from the nature of the problem, that the unknowns are real and that $a > b > c > d > e > 0$. These last restrictions reduce the number of solutions to one. In this first paper the case will be considered, when the slits are smaller than the distances to the neighbouring slits.

To solve the system (3) we suppose

$$a^2 \gg b^2 \gg c^2 \gg d^2 \gg e^2. \qquad (4)$$

This supposition implies $a \gg c \gg e$ and $b \gg d$. Neglecting terms of higher order, the equations (3) simplify considerably. Using the series expansion

$$\ln \frac{a+b}{a-b} = 2\,\frac{b}{a}\left\{1 + \frac{1}{3}\frac{b^2}{a^2} + \frac{1}{5}\frac{b^4}{a^4} + \ldots\right\} \qquad (b<a)$$

we get the approximate equations

$$\left.\begin{aligned} a + 2r_1\frac{b}{a} &= s_1, & 2r_1\frac{c}{b} + 2r_2\frac{d}{c} &= s_2,\\ \frac{a^2}{2b} &= r_1, & \frac{c^2}{2d}\frac{a^2}{b^2} &= r_2,\\ & & 2r_2\frac{e}{d} + \frac{a^2c^2e}{b^2d^2} &= s_3. \end{aligned}\right\} \qquad (5)$$

The exact solution of these approximate equations is

$$\left.\begin{aligned} a &= \frac{s_1}{2}, & b &= \frac{s_1^2}{2^3 r_1} = v_1 a,\\ c &= \frac{s_1^2 s_2}{2^5 r_1^2} = v_2 b, & d &= \frac{s_1^2 s_2^2}{2^7 r_1^2 r_2} = v_3 c,\\ e &= \frac{s_1^2 s_2^2 s_3}{2^9 r_1^2 r_2^2} = v_4 d, \end{aligned}\right\} \qquad (6)$$

the ratios v_n being defined by

$$v_1 = \frac{s_1}{4r_1}; \quad v_2 = \frac{s_2}{4r_1}; \quad v_3 = \frac{s_2}{4r_2}; \quad v_4 = \frac{s_3}{4r_2}.$$

Even more simply these results can be derived directly from the integral (2) using the assumption (4). This will be used in a subsequent paper. The assumption (4) corresponds to $v_n^2 \ll 1$. If we suppose $v_n^2 < 1/10$, this means that the slit widths $2s < 0{,}8\times$ the distances to the neighbouring slits. In most electron lenses this condition will be satisfied.

For symmetrical assemblies, where v_n^2 is no longer small, the corresponding values of a, b, c, d, and e will be calculated in a second paper.

§ 3. Higher approximations and exact solution

Substituting the approximate solution (6) in the original equations (3), we get the slit widths and electrode distances, corresponding to the approximate values of the parameters a to e inclusive.

Supposing $v_n^4 \ll 1$ and neglecting fourth order terms in v_n we get:

$$\begin{aligned} &s_1(1 + \tfrac{1}{6}v_1^2 + \tfrac{1}{2}v_2^2) && \text{instead of } s_1,\\ &r_1(1 - v_1^2 - v_2^2) && \text{instead of } r_1,\\ &s_2(1 + \tfrac{1}{2}v_1^2 + \tfrac{1}{6}v_2^2 + \tfrac{1}{6}v_3^2 + \tfrac{1}{2}v_4^2) && \text{instead of } s_2,\\ &r_2(1 - v_3^2 - v_4^2) && \text{instead of } r_2,\\ &s_3(1 + \tfrac{1}{2}v_3^2 + \tfrac{1}{6}v_4^2) && \text{instead of } s_3, \end{aligned}$$

and this gives an impression of the accuracy obtained with the approximation we have used.

To get better values for the unknowns a, b, c, d, and e, we substitute in the equations (3)

$$\begin{aligned} a &= \tfrac{1}{2}s_1\{1 + A_1 v_1^2 + A_2 v_2^2 + A_3 v_3^2 + A_4 v_4^2\},\\ b &= \tfrac{1}{2}s_1 v_1\{1 + B_1 v_1^2 + B_2 v_2^2 + B_3 v_3^2 + B_4 v_4^2\},\\ c &= \tfrac{1}{2}s_1 v_1 v_2\{1 + C_1 v_1^2 + C_2 v_2^2 + C_3 v_3^2 + C_4 v_4^2\},\\ d &= \tfrac{1}{2}s_1 v_1 v_2 v_3\{1 + D_1 v_1^2 + D_2 v_2^2 + D_3 v_3^2 + D_4 v_4^2\},\\ e &= \tfrac{1}{2}s_1 v_1 v_2 v_3 v_4\{1 + E_1 v_1^2 + E_2 v_2^2 + E_3 v_3^2 + E_4 v_4^2\}. \end{aligned}$$

In the appendix it will be proved, that in the series expansions of the parameters only terms in v_n^2 appear.

In this way it is found:

$$\begin{aligned} &A_1 = -\tfrac{1}{3}; && A_2 = 0; && A_3 = 0; && A_4 = 0;\\ &B_1 = -\tfrac{1}{3}; && B_2 = -1; && B_3 = 0; && B_4 = 0;\\ &C_1 = -\tfrac{4}{3}; && C_2 = -\tfrac{5}{3}; && C_3 = \tfrac{1}{3}; && C_4 = 0;\\ &D_1 = -\tfrac{4}{3}; && D_2 = -\tfrac{4}{3}; && D_3 = -\tfrac{1}{3}; && D_4 = -1;\\ &E_1 = -\tfrac{4}{3}; && E_2 = -\tfrac{4}{3}; && E_3 = -\tfrac{4}{3}; && E_4 = -\tfrac{5}{3}. \end{aligned} \qquad (7)$$

In the same way the fourth order corrections are found to be (Table 1):

	11	12	13	14	22	23	24	33	34	44
A	−4/15	−1	0	0	0	0	0	0	0	0
B	11/45	7/3	0	0	4/3	1/3	0	0	0	0
C	86/45	65/9	−4/9	0	41/15	−1/3	0	−4/15	−1	0
D	86/45	52/9	4/9	4/3	86/45	5/9	4/3	11/45	7/3	4/3
E	86/45	52/9	16/9	20/9	86/45	20/9	20/9	86/45	65/9	41/15

Table 1. Equations (8).

where A_{nm}, B_{nm} etc. are the coefficients of $v_n^2 v_m^2$ for a, b, etc. respectively. This method can be continued to get more accurate values of the parameters.

But if v_n^2 is not very small, the method seems to be tedious and slowly converging (if converging at all). Then an iteration method is more suitable. It may be done in the following way:

The approximate equations (5) are made exact by adding in the right-hand terms the neglected quantities, to get the equations:

$$a + 2\,r_1\,\frac{b}{a} = s_1 - 2\,r_1\,\frac{b}{a}\left\{\frac{1}{3}\,\frac{b^2}{a^2} + \frac{1}{5}\,\frac{b^4}{a^4} + \ldots\right\} - 2\,r_2\,\frac{d}{a}\,(1 + \ldots) - \frac{a\,c^2\,e^2}{b^2\,d^2} = S_1\,,$$

$$\frac{a^2}{2\,b} = r_1\,\frac{b^2-d^2}{b^2-c^2}\,\frac{b^2}{b^2-e^2} + \frac{b}{2} = R_1\,. \qquad (9)$$

$$2\,r_1\,\frac{c}{b} + 2\,r_2\,\frac{d}{c} = s_2 - c - 2\,r_1\,\frac{c}{b}\left\{\frac{1}{3}\,\frac{c^2}{3\,b^2} + \ldots\right\} - 2\,r_2\,\frac{d}{c}\left\{\frac{1}{2}\,\frac{d^2}{c^2} + \ldots\right\} - \frac{a^2\,c\,e^2}{b^2\,d^2} = S_2\,,$$

$$\frac{c^2}{2\,d}\,\frac{a^2}{b^2} = r_2\,\frac{a^2}{a^2-d^2}\,\frac{b^2-d^2}{b^2}\,\frac{d^2}{d^2-e^2} + \frac{a^2}{b^2}\,\frac{d}{2} = R_2\,,$$

$$2\,r_2\,\frac{e}{d} + \frac{a^2\,c^2\,e}{b^2\,d^2} = s_3 - e - 2\,r_1\,\frac{e}{b}\,(1 + \ldots) - 2\,r_2\,\frac{e}{d}\left\{\frac{1}{3}\,\frac{e^2}{d^2} + \ldots\right\} = S_3\,.$$

Now in the right hand terms the approximate values of the unknowns are substituted. With these values $R_{1,2}$ and $S_{1,2,3}$, one gets a more accurate solution of a form analoguous to (6):

$$a = S_1\,\frac{R_1}{r_1 + R_1}\,,$$

$$b = \frac{S_1^2\,R_1}{2\,(r_1+R_1)^2} = a\,V_1\,,$$

$$c = \frac{S_1^2\,S_2\,R_1\,R_2}{4\,(r_1+R_1)^2\,(r_1\,R_2+r_2\,R_1)} = b\,V_2\,,$$

$$d = \frac{S_1^2\,S_2^2\,R_1^2\,R_2}{8\,(r_1+R_1)^2\,(r_1\,R_2+r_2\,R_1)^2} = c\,V_3\,,$$

$$e = \frac{S_1^2\,S_2^2\,S_3\,R_1^2\,R_2}{16\,(r_1+R_1)^2\,(r_1\,R_2+r_2\,R_1)^2\,(r_2+R_2)} = d\,V_4\,,$$

with $V_1 = \dfrac{S_1}{2\,(r_1+R_1)}$; $V_2 = \dfrac{S_2\,R_2}{2\,(r_1\,R_2+r_2\,R_1)}$;

$V_3 = \dfrac{S_2\,R_1}{2\,(r_1\,R_2+r_2\,R_1)}$; $V_4 = \dfrac{S_3}{2\,(r_2+R_2)}$.

These new values of a, b, c, d, and e, substituted in the right-hand terms of (9) furnish more accurate values of $S_{1,2,3}$ and $R_{1,2}$ etc. In practice, this iterating process converges quickly. In this process the correction terms (7) and (8) are not valid.

§ 4. Solution of Laplace's equation in the w-plane

We now have to solve LAPLACE's equation in the w-plane, with the boundary condition the potential distribution along the real axis of the w-plane, corresponding to the given potentials of the electrodes. To achieve this, we discuss at first the potential distribution of Fig. 3 a: along the real axis of the w-plane left of Q $(q, 0)$ the potential is $+1$, right

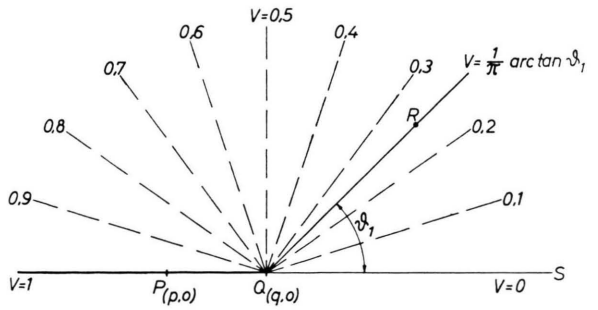

Fig. 3 a.

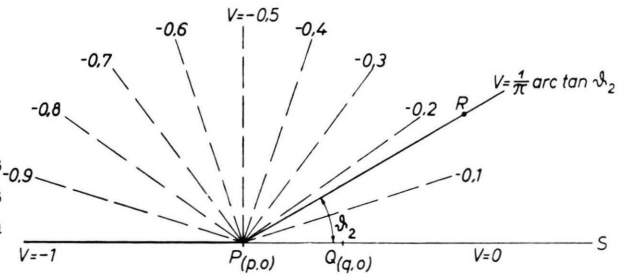

Fig. 3 b.

Fig. 3 a, b. Equipotentials in the w-plane.

of Q zero. It is evident, that the equipotentials in this case are the dotted lines and the potential in a point R is given by $1/\pi < RQS$. From the same reasoning the potential in the point R in the arrangement of Fig. 3 b equals $-1/\pi < RPS$. If the potential distribution along the u-axis is given by:

$$V = 0 \quad \text{for} \quad u < p \quad \text{or} \quad q < u\,,$$
$$V = 1 \quad \text{for} \quad p < u < q\,,$$

the potential in $R(u, v)$ may be found by linear superposition of the above cases. In our notation this corresponds to

$$V(u, v) = 1/\pi\left\{\arctan\frac{v}{u-q} - \arctan\frac{v}{u-p}\right\} \qquad (10)$$

where the arc tan should be chosen in accordance with the boundary conditions. When

$$\arctan\frac{v}{u-q} \to 0 \quad \text{for} \quad v \to 0 \quad \text{and} \quad u > q\,,$$

$$\arctan\frac{v}{u-p} \to 0 \quad \text{for} \quad v \to 0 \quad \text{and} \quad u > p\,.$$

$V(u, 0)$ satisfies the boundary condition.

The equations (2) and (10) give in an implicit form the potential in the slit system.

Most interesting, however, is the potential distribution along the central line of the lens system. This line coincides with the imaginary axis. Using the

identity

$$\ln \frac{p+q\,i}{p-q\,i} = 2\,i \arctan \frac{q}{p},$$

equation (2) transforms into

$$y = \frac{z}{i} = v - 2\,B \arctan \frac{v}{b} - 2\,D \arctan \frac{v}{d} - \frac{E}{v}$$

for points on the imaginary axis. Similarly for these points (10) transforms into

$$V(v) = \frac{1}{\pi}\left\{\arctan \frac{v}{p} - \arctan \frac{v}{q}\right\}$$

again giving in an implicit form the potential distribution along the central line.

Near the main axis of the slit lens the potential distribution can be computed by series expansion:

$$V(x,y) = V(0,y) + \left(\frac{\partial V}{\partial x}\right)_{0,y} x + \frac{1}{2}\left(\frac{\partial^2 V}{\partial x^2}\right)_{0,y} x^2 + \cdots .$$

In the case of a symmetrical potential distribution all odd derivatives are zero. According to (1)

$$\frac{\partial^2 V}{\partial x^2} = -\frac{\partial^2 V}{\partial y^2};$$

by differentiation all even derivatives can be found:

$$\frac{\partial^4 V}{\partial x^4} = \frac{\partial^4 V}{\partial y^4} \quad \text{etc.}$$

So from the known potential distribution along the central line the potential near this line is given by:

$$V(x,y) = V(0,y) - \frac{1}{2!}x^2 V_{yy}(0,y) + \frac{1}{4!}x^4 V_{yyyy}(0,y) - + \cdots .$$

§ 5. Example

As an example we take the slit lens represented in Fig. 4. The units are arbitrary.

From the values

$$s_1 = 0.5; \quad s_2 = 1; \quad s_3 = 0.75; \quad r_1 = r_2 = \frac{3}{\pi} = 0.954930$$

we get in the successive approximations (s. Table 2).

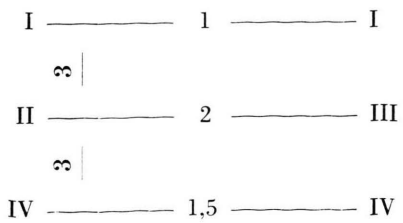

Fig. 4. Example.

	form. (6)	first approx. (7)	second approx. (8)	
a	0.250000	0.251428	0.251115	
$10b$	0.327249	0.302951	0.306527	
$100c$	0.856736	0.758870	0.772491	
$100d$	0.224293	0.184900	0.192382	
$1000e$	0.440398	0.321547	0.351633	
	first iteration from (7)	second iteration	third iteration	fourth iteration
a	0.251374	0.251119	0.251177	0.251170
$10b$	0.306646	0.305802	0.305939	0.305919
$100c$	0.772408	0.770376	0.770781	0.770737
$100d$	0.192341	0.190875	0.191111	0.191081
$1000e$	0.349595	0.344906	0.345585	0.345495

Table 2.

From these diverse approximations we get the following slit widths and electrode distances, using the formulae (3) (s. Table 3).

	nominal value	form. (6)	first approx.	fourth iteration
$2s_1$	1.000000	1.038	0.994	1.000000
πr_1	3.000000	2.759	3.038	2.999992
$2s_2$	2.000000	2.103	1.974	2.000040
πr_2	3.000000	2.699	3.085	3.000029
$2s_3$	1.500000	1.562	1.458	1.499988

Table 3.

In Table 4 various potential distributions are given along the axis of the system, when the indicated electrode has the potential 1. When the electrodes have different potentials, the potential distribution is a linear superposition. In Table 5 the corresponding fields along the axis are given. In the second and last columns the case is given, when there are no potentials on the electrodes but a field of 1 unit of field strength is applied before resp. behind the lens. In the Figs. 5 and 6 the results are represented graphically.

This theory has been developed for lens systems with electrodes of infinitely small thicknesses. In most cases there is an equipotential in the neighbourhood of the infinitely thin electrodes corresponding in fair approximation to the form of the actual electrodes of finite thickness with rounded edges as indicated in Fig. 7. Thus real cases can also be treated with this theory, if we change in the right way the position of the electrode, the slit width, and the potential of the electrode.

Appendix

Proof, that only terms in v_n^2 appear in the series expansions of the parameters a, b, c, d, and e.

The proof is given by induction. The defining for-

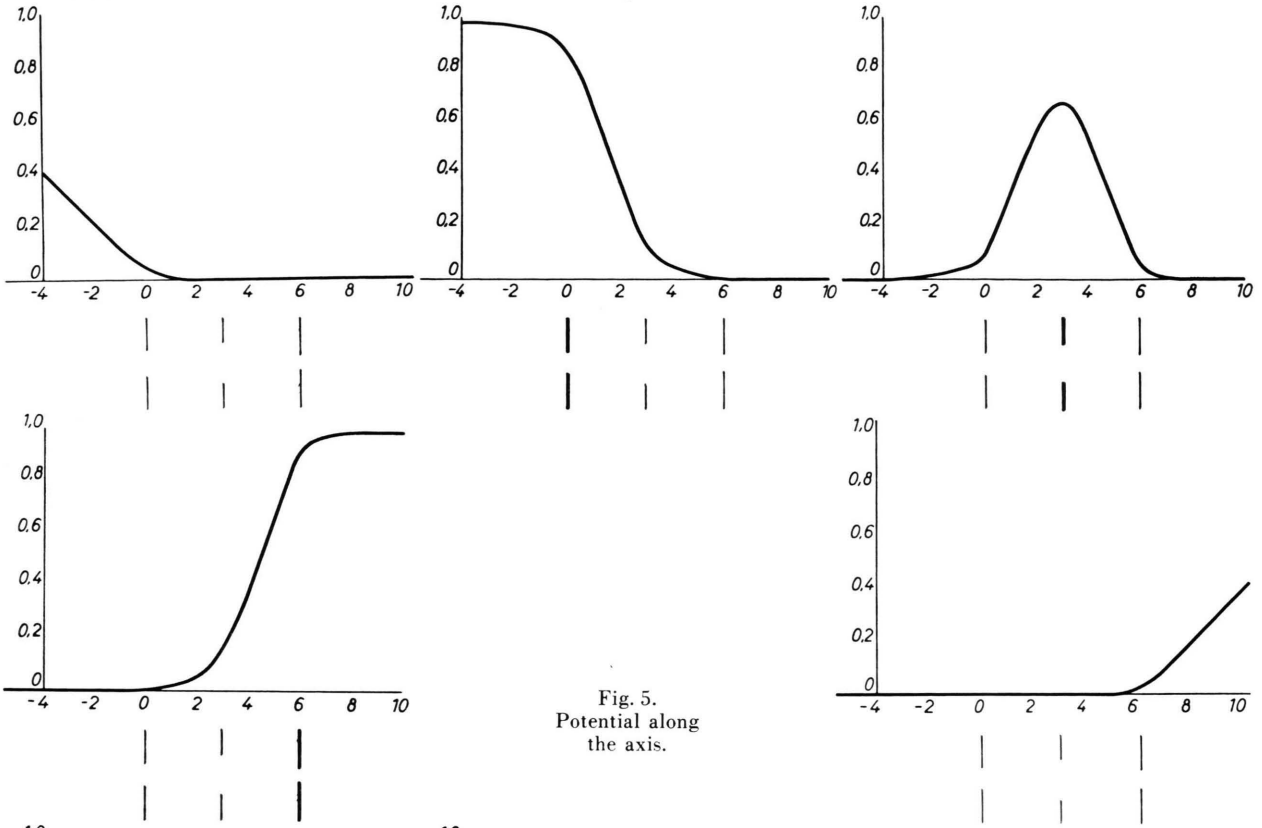

Fig. 5.
Potential along
the axis.

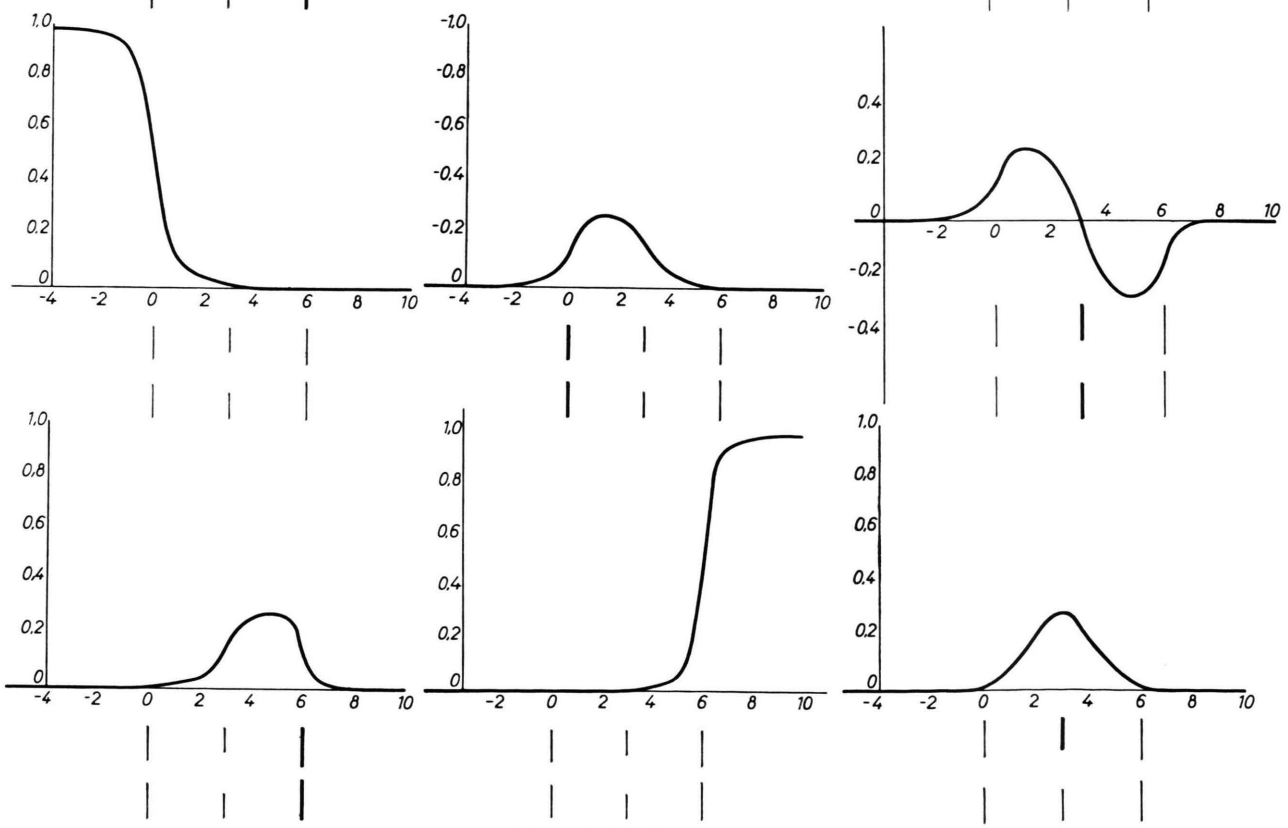

Fig. 6. Field along the axis.

y	$V(y)$ (1)	$V(y)$ (2)	$V(y)$ (3)	$V(y)$ (4)	$V(y)$ (5)
−130.9	130.9	0.999667	0.000312	0.000021	0.000001
− 65.5	65.5	0.999333	0.000626	0.000041	0.000002
− 26.18	26.19	0.998334	0.001562	0.000104	0.000005
− 13.08	13.09	0.996669	0.003123	0.000208	0.000010
− 6.524	6.546	0.993337	0.006247	0.000416	0.000020
− 2.565	2.618	0.98335	0.01561	0.001040	0.000050
− 1.203	1.309	0.96672	0.03120	0.002081	0.000100
− 0.443	0.6546	0.93361	0.06223	0.004162	0.000200
0.259	0.2618	0.83707	0.15243	0.010505	0.000500
0.853	0.13091	0.6931	0.2861	0.02080	0.001000
1.605	0.06546	0.4855	0.4730	0.04156	0.002000
2.591	0.02618	0.2324	0.6645	0.10313	0.005000
3.240	0.013091	0.12020	0.6787	0.20113	0.010000
3.937	0.006546	0.06064	0.5707	0.3686	0.020000
4.926	0.002618	0.02432	0.3252	0.6504	0.05000
5.495	0.001309	0.01216	0.17683	0.81100	0.10000
5.891	0.000655	0.006082	0.09055	0.90337	0.20000
6.376	0.000262	0.002433	0.03647	0.96110	0.5000
6.938	0.000131	0.001216	0.01826	0.93053	1.0000
7.969	0.000066	0.000608	0.009130	0.990262	2.0000
10.99	0.000026	0.000243	0.003652	0.996105	5.0000
15.99	0.000013	0.000122	0.001826	0.998052	10.000
26.00	0.000007	0.000061	0.000913	0.999026	20.000

Tab. 4. Potentials along the axis of the lens of Fig. 4.

(1) external field lefthand side of the lens.
(2) first electrode potential + 1.
(3) second electrode potential + 1.
(4) third electrode potential + 1.
(5) external field righthand side of the lens.

y	$\frac{\delta V}{\delta y}$ (6)	$\frac{\delta V}{\delta y}$ (7)	$\frac{\delta V}{\delta y}$ (8)	$\frac{\delta V}{\delta y}$ (9)	$\frac{\delta V}{\delta y}$ (10)	$\frac{\delta V}{\delta x}$ (11)
−130.9	−0.999992	0.000003	0.000002	0.000000	0.000000	0.000000
− 65.5	−0.999968	0.000010	0.000010	0.000001	0.000000	0.000000
− 26.18	−0.999797	0.000064	0.000060	0.000004	0.000000	0.000000
− 13.08	−0.999189	0.000254	0.000238	0.000016	0.000001	0.000001
− 6.524	−0.996763	0.001015	0.000951	0.000063	0.000003	0.000005
− 2.565	−0.980118	0.006230	0.005842	0.000388	0.000019	0.000081
− 1.203	−0.92508	0.02348	0.02201	0.001471	0.000071	0.000612
− 0.443	−0.7567	0.07620	0.07139	0.004812	0.000231	0.003972
+ 0.259	−0.3439	0.20480	0.19114	0.013664	0.000657	0.02668
0.853	−0.13374	0.26718	0.24594	0.02124	0.001022	0.06956
1.605	−0.05713	0.27754	0.24136	0.03617	0.001746	0.14406
2.591	−0.026935	0.21839	0.11413	0.10426	0.005144	0.27720
3.240	−0.013939	0.12496	−0.07522	0.20018	0.010647	0.29426
3.937	−0.006049	0.05570	−0.21376	0.26946	0.018483	0.20341
4.926	−0.002683	0.02490	−0.26556	0.29046	0.05124	0.08838
5.495	−0.001948	0.018094	−0.24690	0.26499	0.14880	0.04036
5.891	−0.001298	0.012059	−0.17660	0.18866	0.39655	0.014371
6.376	−0.000420	0.003899	−0.05829	0.06219	0.80131	0.001895
6.938	−0.000123	0.001145	−0.017173	0.018319	0.941485	0.000279
7.969	−0.000032	0.000299	−0.004494	0.004793	0.984690	0.000037
10.99	−0.000005	0.000049	−0.000729	0.000777	0.997518	0.000002
15.99	−0.000001	0.000012	−0.000182	0.000195	0.999378	0.000000
26.00	−0.000000	0.000003	−0.000046	0.000049	0.999845	0.000000

Tab. 5. Fields along the axis of the lens of Fig. 4.

(6) external field lefthand side of the lens.
(7) first electrode potential + 1.
(8) second electrode potential + 1.
(9) third electrode potential + 1.
(10) external field righthand side of the lens.
(11) cross-field, when half of the second electrode potential + 1.

mulae (6) of the v_n include that

$$r_1 = \frac{s_1}{4\,v_1}\,; \quad s_2 = \frac{v_2}{v_1}\,s_1\,; \quad r_2 = \frac{v_2}{4\,v_1\,v_3}\,s_1\,; \quad s_3 = \frac{v_2\,v_4}{v_1\,v_3}\,s_1\,,$$

so the five quantities s_1, r_1, s_2, r_2 and s_3 determining the values of the unknowns a, b, c, d, and e can be replaced by s_1, v_1, v_2, v_3, and v_4. If in the formulae (3) all parameters a, b, c, d, and e are multiplied by the same factor, also the quantities s_1, r_1, s_2, r_2, and s_3 are multiplied by this same factor.

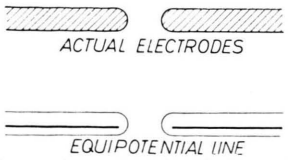

Fig. 7. Comparison of real and theoretical cases.

These two facts imply that the following series expansions are valid:

$$a = s_1 \sum a_{klpq}\, v_1{}^k\, v_2{}^l\, v_3{}^p\, v_4{}^q$$

and analoguous for b, c, d, and e. In § 1 the first terms of these expansions have been found, and the expansion for b gets the more special form

$$b = \tfrac{1}{2}\, s_1\, v_1 \sum b_{klpq}\, v_1{}^k\, v_2{}^l\, v_3{}^p\, v_4{}^q$$

and analoguous for c, d, and e.

By substituting the series expansions of the parameters a, b, c, d, and e with only first order terms in v_n included $(k+l+p+q=1)$ in the formulae (3), it is easily proved, that these first order terms are all zero.

Now we suppose, that we have the series expansions up to the $(2n+1)^{\text{st}}$ order:

$$a = \tfrac{1}{2}\, s_1 (1 + A_{2n} + a_{2n}) ,$$

$$b = \tfrac{1}{2}\, s_1\, v_1 (1 + B_{2n} + b_{2n}) \text{ etc.}$$

where A_{2n}, B_{2n}, etc. contain only even powers of the v_k up to the order $2n$ and a_{2n} or b_{2n} etc. is the term of lowest order, having odd powers of one or more of the v_k, this order thus being $2n$ or $2n+1$. Evaluating

$$a^2, \quad a^2 - b^2, \quad a^2/b^2, \quad r_1 (b/a)^{2m+1}, \quad \text{etc.}$$

which are in fact the only expressions, occurring in the equations (3) after performing the series expansions for the logarithms, one will find that odd terms of the order $2n$ or $2n+1$ only enter as homogeneous first order expressions in a_{2n}, b_{2n} etc. Equating all terms of this order to zero, provides:

$$a_{2n} = b_{2n} = \ldots = 0 .$$

The author wishes to thank Prof. Dr. J. KISTEMAKER for his stimulating interest in this calculations, Mr. H. A. TASMAN for valuable discussions and Mr. M. P. PULLIN for checking the manuscript.

This work is part of the research program of the Stichting voor Fundamenteel Onderzoek der Materie and was made possible by financial support from the Nederlandse Organisatie voor Zuiver Wetenschappelijk Onderzoek.

Shape of the Magnetic Field between Conical Pole Faces

By A. J. H. BOERBOOM and H. A. TASMAN

Laboratorium voor Massaspectrografie, Amsterdam, The Netherlands

and H. WACHSMUTH

Physikalisches Institut der Technischen Hochschule, München

(Z. Naturforschg. **14 a**, 816—818 [1959]; eingegangen am 14. Juni 1959)

Calculation is made of the shape of the magnetic field between conical pole faces, which may be used as an inhomogeneous deflecting field for a mass spectrometer. The results are expressed as a series expansion in the coordinates around the main path, and in the gap width at the radius of the main path.

The application of ψ-independent, inhomogeneous magnetic deflecting fields for mass spectrometers offers the possibility of considerable increase in resolving power without increase of radius or decrease of slit widths (TASMAN and BOERBOOM [1]; WACHSMUTH, BOERBOOM and TASMAN [2]; TASMAN, BOERBOOM and WACHSMUTH [3]). Hereto magnetic fields are required, which decrease with increasing radius. The simplest way to create such fields is the use of conical pole faces, between which the gap increases with increasing radius. The present calculations provide the shape of the resulting field, as a power expansion in the normal and binormal coordinates, and the gap width at the radius r_m of the main path, for the symmetrical case with respect to the median plane.

The coordinate system is shown in Fig. 1; a radial section is represented in Fig. 2. Use is made of the dimensionless coordinates: normal coordinate $u = (r - r_m)/r_m$; binormal coordinate $v = z/r_m$; path coordinate $w = \psi$. The gap width at $u = 0$ equals $2\, b\, r_m$.

1. The scalar magnetic potential

The scalar magnetic potential φ_m is related to the magnetic field strength $\mathfrak{B}$ through its definition:

[1] H. A. TASMAN and A. J. H. BOERBOOM, Z. Naturforschg. **14 a**, 121 [1959].

[2] H. WACHSMUTH, A. J. H. BOERBOOM and H. A. TASMAN, Z. Naturforschg. **14 a**, 818 [1959].

[3] H. A. TASMAN, A. J. H. BOERBOOM and H. WACHSMUTH, Z. Naturforschg. **14 a**, 822 [1959].